



HAL
open science

A mycolyl transferase mutant of lacking capsule integrity is fully virulent

Tobias Sydor, Kristine von Bargaen, Ulrike Becken, Sabine Spuerck, Vivian M. Nicholson, John F. Prescott, Albert Haas

► **To cite this version:**

Tobias Sydor, Kristine von Bargaen, Ulrike Becken, Sabine Spuerck, Vivian M. Nicholson, et al.. A mycolyl transferase mutant of lacking capsule integrity is fully virulent. *Veterinary Microbiology*, 2008, 128 (3-4), pp.327. 10.1016/j.vetmic.2007.10.020 . hal-00532345

HAL Id: hal-00532345

<https://hal.science/hal-00532345>

Submitted on 4 Nov 2010

HAL is a multi-disciplinary open access archive for the deposit and dissemination of scientific research documents, whether they are published or not. The documents may come from teaching and research institutions in France or abroad, or from public or private research centers.

L'archive ouverte pluridisciplinaire **HAL**, est destinée au dépôt et à la diffusion de documents scientifiques de niveau recherche, publiés ou non, émanant des établissements d'enseignement et de recherche français ou étrangers, des laboratoires publics ou privés.

Accepted Manuscript

Title: A mycolyl transferase mutant of *Rhodococcus equi* lacking capsule integrity is fully virulent

Authors: Tobias Sydor, Kristine von Bargaen, Ulrike Becken, Sabine Spuerck, Vivian M. Nicholson, John F. Prescott, Albert Haas



PII: S0378-1135(07)00525-1
DOI: doi:10.1016/j.vetmic.2007.10.020
Reference: VETMIC 3861

To appear in: *VETMIC*

Received date: 25-7-2007
Revised date: 18-10-2007
Accepted date: 19-10-2007

Please cite this article as: Sydor, T., von Bargaen, K., Becken, U., Spuerck, S., Nicholson, V.M., Prescott, J.F., Haas, A., A mycolyl transferase mutant of *Rhodococcus equi* lacking capsule integrity is fully virulent, *Veterinary Microbiology* (2007), doi:10.1016/j.vetmic.2007.10.020

This is a PDF file of an unedited manuscript that has been accepted for publication. As a service to our customers we are providing this early version of the manuscript. The manuscript will undergo copyediting, typesetting, and review of the resulting proof before it is published in its final form. Please note that during the production process errors may be discovered which could affect the content, and all legal disclaimers that apply to the journal pertain.

1 **A mycolyl transferase mutant of *Rhodococcus equi***
2 **lacking capsule integrity is fully virulent**

3
4
5
6
7
8 Tobias Sydor¹, Kristine von Bargaen¹, Ulrike Becken¹, Sabine Spuerck¹,
9 Vivian M. Nicholson², John F. Prescott², and Albert Haas^{1,#}

10 Institute for Cell Biology and Bonner Forum Biomedizin, University of Bonn, Ulrich-
11 Haberland-Str. 61a, 53121 Bonn, Germany¹, and Department of Pathobiology,
12 University of Guelph, Guelph, Ontario N1G 2W1, Canada²

13
14
15
16 # Corresponding author

17
18 Dr. Albert Haas
19 Cell Biology Institute
20 University of Bonn
21 Ulrich-Haberland-Str. 61a
22 53121 Bonn
23 Germany
24 tel. ++49 228 736340
25 fax ++49 228 736304
26 albert.haas@uni-bonn.de
27

28
29 **Running title:** *Rhodococcus equi* mycolyltransferase

30
31 **Abbreviations:** BMM, bone marrow-derived macrophages; MOI, multiplicity of
32 infection; ORF, open reading frame; RCV, *R. equi*-containing vacuole; VAP,
33 virulence-associated plasmid; TDM, trehalose dimycolate; VapA, virulence-
34 associated protein A; BHI: brain heart infusion

35 **ABSTRACT**

36 *Rhodococcus equi* is a mucoid Gram-positive facultative intracellular pathogen which
37 can cause severe bronchopneumonia in foals and AIDS patients. A polysaccharide
38 capsule which gives *R. equi* a mucoid appearance has long been suspected to be a
39 virulence factor. Here, we describe a transposome mutant in the gene *fbpA* of strain
40 *R. equi* 103 which caused absence of a capsular structure. *FbpA* is a chromosomal
41 gene homologous to antigen 85 (Ag85) mycolyl chain transferase gene of
42 *Mycobacterium tuberculosis*. The mutant multiplied normally in isolated
43 macrophages, was able to establish the unusual *R. equi*-containing vacuole in
44 macrophages, was cytotoxic for macrophages, and was virulent in a mouse model.
45 Colonies had a dry appearance on nutrient agar and defective capsule structure.
46 Surprisingly, *fbpA* mutants cured of the virulence-associated plasmid were found in a
47 phagosome that was more alkaline than the corresponding wild-type bacteria, and
48 were more cytotoxic and even multiplied to some extent. This study suggests that the
49 capsule is not an important virulence factor of *R. equi* and that it may even
50 counteract virulence traits.

51

52

53 **Key words:** pneumonia, phagosome, mycolyl transferase, capsule, *Mycobacterium*,

54 *Rhodococcus*

55

56

57 **INTRODUCTION**

58

59 *Rhodococcus equi* is a nocardioform Gram-positive coccobacillus, closely related to
60 mycobacteria, and an important foal pathogen producing severe pyogranulomatous
61 pneumonia in very young horses and tuberculosis-like symptoms in AIDS patients
62 (Donisi et al., 1996).

63 *R. equi* is a facultative intracellular bacterium (Zink et al., 1987;
64 Hondalus and Mosser, 1994) which interferes with the maturation of its phagosomes
65 in macrophages (Fernandez-Mora et al., 2005): Phagosomes containing virulent *R.*
66 *equi* run normally through the early phagocytic stages, yet arrest phagosome
67 maturation before turning into phagolysosomes, leaving them non-acidified and
68 without lysosomal cathepsin hydrolases (Fernandez-Mora et al., 2005). Both the
69 abilities to change phagosome maturation and to eventually kill the host cell by
70 necrosis (Lührmann et al., 2004) are regulated by a virulence-associated plasmid
71 (VAP) of 80-90 kbp found in most clinical isolates from foals. It mediates the
72 expression of the 'virulence-associated plasmid protein A' (VapA), a secreted
73 virulence-related lipoprotein and a phenotypic marker of this plasmid (Tan et al.,
74 1995; Jain et al., 2003).

75 One of the suggested virulence factors of *R. equi* is the possession of a
76 polysaccharide capsule forming 27 serotypes (Hondalus, 1997; Prescott, 1991).
77 There is no strict correlation between serotype and virulence, although the serotypes
78 1 and 2 are the most frequent among clinical isolates (Prescott, 1981; Takai et al.,
79 1991), leaving the possibility that *R. equi* capsules serve multiple purposes. Here, we
80 have isolated capsule-deficient mutants from a transposome mutant library of *R. equi*
81 which were then analysed for virulence functions.

82 **MATERIALS AND METHODS**

83 All chemicals used in this study were from Sigma-Aldrich (Taufkirchen, Germany)
84 unless stated otherwise.

85

86 **Cells**

87 *Rhodococcus equi* 103+ (capsular serotype 6) was originally isolated from a
88 pneumonic foal (De la Pena-Moctezuma and Prescott, 1995a) and was grown in
89 brain heart infusion (BHI, Difco) broth or minimal medium (Ashour et al., 2003) with
90 trace metal solution (Vishniac and Santer, 1957) using 20 mM acetate as a carbon
91 source at 30 or 37°C on a rotary shaker at 190 rpm or on BHI nutrient agar.
92 *Escherichia coli* XL-1Blue cells were grown in Luria Bertani (LB, Roth, Karlsruhe,
93 Germany) agar or broth at 37°C and 190 rpm. Antibiotics were used at 50µg/ml
94 (kanamycin / *E. coli*), 100 µg/ml (hygromycin / *R. equi*, Invitrogen, Carlsbad,
95 Germany), or 200 µg/ml (kanamycin / *R. equi*). To cure *R. equi* of the virulence-
96 associated plasmid, bacteria were grown at 37°C in broth for 2-3 weeks with sub-
97 culturing every 2 days. Loss of the virulence-associated plasmid in single clones was
98 assayed by immuno-dot blot using the monoclonal VapA antibody 10G5 (Takai et al.,
99 1995). All plasmids, strains, and oligonucleotides are summarized in Table I. Mouse
100 macrophages (J774E cell line and bone marrow derived macrophages [BMMs]) were
101 prepared as in Fernandez-Mora et al. (2005). Microscopic quantification of bacterial
102 counts using SYTO13 was done as described in Pei et al. (2006). For the
103 sedimentation assay, bacteria were grown as above for 16h and tubes were left
104 standing in a tube rack at ambient temperature for 24 h.

105

106 ***R. equi* transposome mutants**

107 Electro-competent *R. equi* were prepared as published (Sekizaki et al., 1998).
108 Transposome-mutagenesis of *R. equi* 103+ was done by using the EZ::TN <KAN-2>
109 Tnp Transposome Kit (Epicentre Biotechnologies, Hess, Germany) (Mangan and
110 Meijer 2001). In brief, 20 ng transposome was mixed with 100 µl of electro-competent
111 *R. equi*-solution (10^{10} cells) using a Micro-Pulser (2.5 kV; 800 Ω 5.2 ms) (Biorad,
112 München, Germany). Selection was on LB agar containing 200 µg kanamycin per ml
113 and incubation for 2-3 days at 30°C. Identification of integration site: Bacterial
114 genomic DNA was extracted using the Qiagen (Hilden, Germany) 500 tip genomic
115 DNA extraction kit, digested with *KpnI*, and ligated into *KpnI*-digested pBluescript II
116 (SK+) (Stratagene, La Jolla, California) and used to transform *E. coli* XL1-Blue.
117 Transposome-containing clones were selected on LB nutrient agar with kanamycin.
118 Plasmid DNA of positive clones was extracted using the Qiagen Miniprep kit and
119 sequenced by GATC-Biotech (Konstanz, Germany) using specific primers provided
120 with the EZ::TN <KAN-2> Tnp Transposome Kit. The obtained sequences were
121 compared with sequences in the Sanger Institute Date Base. These sequence data
122 were produced by the *Rhodococcus equi* Sequencing Group at the Sanger Institute
123 and can be obtained from <ftp://ftp.sanger.ac.uk/pub/pathogens/re/>.

124

125 **Complementation of *R. equi* transposome mutants and Southern blotting**

126 Transposome-containing DNA fragments cloned as described above were amplified
127 by PCR using specific primers that included cleavage sites for restriction enzymes
128 *XbaI* or *ClaI* (forward primer [*fbpA* FP] and reverse primer [*fbpA* RP], Tab. 1). PCR-
129 fragments were digested, ligated into the shuttle vector pSMT3 (Herrmann et al.,
130 1996) to transform *E. coli* XL-1Blue cells with selection on LB agar/hygromycin. DNA
131 of clones growing on hygromycin was extracted and electroporated into *R. equi*.
132 Southern blot analysis was with bacterial genomic DNA, extracted with the GenElute

133 Bacterial Genomic DNA Kit (Sigma-Aldrich Taufkirchen, Germany) and *EcoRI*
134 digested. Detection on nylon membranes (Roche, Mannheim, Germany) was done
135 using the DIG High Prime DNA Labeling and Detection Starter Kit II (Roche). A 1,109
136 bp PCR fragment of the transposome sequence was amplified using specific primers
137 (forward primer [Tn FP] and reverse primer [Tn RP], Tab. 1) labelling, hybridisation,
138 and chemiluminescence detection were done according to the manufacturer's
139 instructions.

140

141 **Nigrosin/eosin negative stain**

142 Five μl of a bacterial suspension in PBS were mixed with 5 μl of a 5% eosin-solution
143 and incubated for 3 min. Five μl of a 5% nigrosin solution were added and the fluid
144 was spread to a thin layer using a second slide. Slides were air-dried and examined
145 with a Zeiss Axioplan light microscope using the 100 x oil immersion objective.

146

147 **FRET-based phagosome/lysosome-fusion assay**

148 To quantify phagosome-lysosome fusion, lysosomes of macrophages were
149 preloaded with BSA-rhodamine (acceptor fluorophor) and cells were subsequently
150 infected with ATTO488 (donor-fluorophor) labeled bacteria as described in the
151 following sections. As controls, each experiment contained additionally one sample
152 with uninfected cells but with rhodamine labeled lysosomes ('acceptor only'), and one
153 sample infected with prelabeled bacteria but without BSA-rhodamine ('donor only').
154 Rhodamine-labeled BSA was prepared by dissolving 5 mg of BSA in 1 ml 0.1 M
155 NaHCO_3 with 240 μl NHS-tetramethylrhodamine as follows: 5 mg carboxytetramethyl
156 rhodamine (Molecular Probes, Eugene, USA) were mixed with 10 mg *N*-
157 hydroxysuccinimide and 12 mg carbodiimide in 1 ml DMF. The solution was mixed
158 slowly for 2 h at room temperature. Aggregates were removed by centrifugation at

159 16,000 g for 30 min. Unbound dye and DMF were removed by filtration through a
160 Sephadex G 25 column equilibrated with PBS.

161 To label lysosomes, J774E-macrophages were grown in 12-well plates for 2 days
162 before infection, medium was replaced by medium containing 150 µg BSA-
163 rhodamine per ml, and cells were incubated for 1 h to label the endocytic system.
164 Cells were washed 3 times in pre-warmed PBS and the fluor was chased into
165 lysosomes for 2 h in DMEM/10% FCS at 37°C. Bacteria were grown at 37°C to late
166 logarithmic phase and 1.5 ml of the culture was centrifuged for 5 min at 6,200 g.
167 Bacteria were washed twice with PBS and once with 0.1 M NaHCO₃ (pH 8.3),
168 harvested by centrifugation for 5 min at 6,200 g, resuspended in 50 µl 0.1 M NaHCO₃
169 containing 50µg/ml ATTO488-NHS (Attotec, Siegen, Germany), and incubated for 1
170 h at room temperature in the dark. Bacteria were washed once with PBS,
171 resuspended in 1 ml of 20 mM Tris/HCl and incubated for 10 min at room
172 temperature. Finally, bacteria were washed twice and resuspended in PBS.
173 Macrophages were infected with ATTO488-labeled *R. equi* at 30 bacteria per
174 macrophage for 30 min at 37°C. Unbound bacteria were removed by rinsing 3 times
175 with PBS. Incubations were continued for 90 min at 37°C. Macrophages were
176 harvested by rinsing once with warm PBS, followed by 1 ml ice-cold PBS/5mM EDTA
177 for 5 minutes and pipetting media up and down. Cells were transferred to microfuge
178 tubes, collected by centrifugation for 5 min at 160 g, resuspended in 200 µl PBS, and
179 190 µl of the solution was placed in a well of a 96-well plate. FRET was calculated
180 from fluorescence readout from a FLx800 microplate fluorescence reader (Biotec,
181 Bad Friedrichshall, Germany). The settings were: green excitation 485/20 nm,
182 emission 516/20 nm, red excitation 560/40 nm, emission 635/32 nm, FRET excitation
183 485/20 nm, emission 635/32nm. Obtained FRET values were corrected with a
184 method modified from Yates et al. (2005) using the controls “only red’ and ‘only

185 green' and were indicated as FRET/green ratio (FRET signal per amount of bacteria).
186 The excitation and emission spectra of tetramethylrhodamine and ATTO488 overlap
187 slightly. 'False fret' (F) due to direct excitation of the acceptor at 485 nm (F_A) and due
188 to donor emission at 635 nm (F_D) was calculated using the 'acceptor only' and the
189 'donor only' controls: $F_A = \text{fret ('acceptor only')} / \text{red ('acceptor only')}$; $F_D = \text{fret ('donor$
190 $\text{only')} / \text{green ('donor only')}$; F_A and F_D are means of duplicates. For the samples
191 containing both prelabeled lysosomes and labeled bacteria 'false FRET' was
192 deducted from the measured FRET values using the following equation: $\text{FRET}_{\text{CORR}} =$
193 $\text{fret ('sample')} - F_A * \text{red ('sample')} - F_D * \text{green ('sample')}$. Corrected FRET signals
194 were indicated as FRET signal per amount of bacteria: $\text{FRET}_{\text{CORR}} / \text{green ('sample')}$.
195 $\text{FRET}_{\text{CORR}} / \text{green ('sample')}$ was expressed as mean of duplicates. In each
196 experiment $\text{FRET}_{\text{CORR}} / \text{green}$ for the sample containing *R.equi* 103+/fbpA+ was set
197 to 1.

198

199 **Cytotoxicity of *R. equi* strains for murine J774E macrophages**

200 Infection of macrophages was carried out as described (Lührmann et al., 2004).
201 Cytotoxicity was analysed by quantifying the enzymatic activity of released cytosolic
202 lactate dehydrogenase using the Cytotoxicity Detection Kit (Roche) as in Pei et al.
203 (2006) modified as follows: after infection, medium containing 150 µg gentamicin
204 sulphate per ml was added for 1 h to kill extracellular bacteria, medium was then
205 replaced by medium containing 10 µg gentamicin sulphate per ml and incubated at
206 37°C for an additional 23 h.

207

208 **Extraction of bacterial lipids and TLC analysis**

209 The bacteria from a 150 ml BHI broth culture grown at 37°C to a late-log phase were
210 harvested by centrifugation and washed once in PBS. Bacterial lipids were extracted

211 by resuspending the bacteria in 6 ml chloroform/methanol (2:1; v/v) (Roth, Karlsruhe,
212 Germany), sonication for 5 min and mixing on a magnetic stirrer for 1 h at ambient
213 temperature. Organic phases were separated by centrifugation for 15 min at 1,800 g,
214 collected and the interphase was redissolved in 6 ml chloroform/methanol (1:2; v/v),
215 sonicated for 5 min and again stirred for 1 h at ambient temperature. After
216 centrifugation, the organic phases were pooled with the previously obtained phases
217 and the solvent was evaporated with a stream of nitrogen. The crude lipid extract
218 was re-dissolved in chloroform/methanol (1:1; v/v), equal amounts (200 µg) were
219 separated on TLC plates (Merck, Darmstadt, Germany) using chloroform/methanol
220 (9:1; v/v) as a solvent, and lipids were visualized with CuSO₄/phosphoric acid and
221 heating at 250°C (Yao and Rastetter, 1985).

222

223 **Measurement of phagosome pH in J774E cells**

224 Phagosome pH was determined using a ratiometric system. Two fluorophores were
225 coupled onto the bacterial surface before infection: One whose fluorescence
226 emission is independent of pH (rhodamine, TAMRA) and one whose emission
227 strongly depends on pH (carboxyfluorescein, CF). The pH-independent fluorophore
228 quantifies ingested particles, the pH-dependent fluorophore indicates pH (Li et al.,
229 2005). J774E cells were seeded in 24-well plates at a density of 1.5×10^5 cells per
230 well in DMEM/FCS and incubated for 2 days at 37°C, 7% CO₂. Bacteria were grown
231 in BHI over night, harvested and labeled with TAMRA (0.1 µg/ml) and CF (0.15
232 µg/ml) for 30 min on ice in 0.1 M NaHCO₃. The reaction was quenched with Tris-HCl
233 (pH 8) and the bacteria were washed twice with PBS. Labeling did not affect bacterial
234 viability (not shown). Before infection, 2.5×10^8 fluorescently labeled bacteria per ml
235 were suspended in DMEM/FCS at 37°C in a water bath and macrophages mixed with
236 200 µl of this suspension for 15 min at 37°C, 7% CO₂, followed by 3 rinses with PBS

237 and addition of fresh medium. For *in situ* calibration, infected macrophages were
238 incubated for 1 h (37°C, 7% CO₂): Slides were rinsed twice with PBS, and 500 µl of
239 calibration buffer (buffer adjusted to different pH containing 50 mM additional KCl and
240 10 µM nigericin) were added. Wells of uninfected cells in assay buffer (buffer of
241 neutral pH containing additional 50 mM KCl and 1% methanol) were used as blank.
242 Samples were measured after 20 min incubation at room temperature in a FLx800
243 Multi-Detection Microplate Reader (BioTek, Bad Friedrichshall). Excitation/Emission
244 was 488 nm/516 nm (CF) and 520 nm/635 nm (TAMRA), respectively. The
245 CF/TAMRA fluorescence intensity ratios were plotted against pH. An *in situ*
246 calibration was carried out for each experiment.

247

248 **Test for virulence in a mouse model**

249 Virulence of 103+/fbpA+, 103-/fbpA+, 103+/fbpA-, and 103-/fbpA- was tested in a
250 CD1 mouse liver clearance model (day 4 post infection) as described previously (Pei
251 et al., 2006).

252

253 **Transmission and scanning electron microscopy**

254 For transmission electron microscopy *R. equi* were grown on BHI-agar at 37°C for 2
255 days, scraped off and resuspended in 1 ml PBS. Bacteria were pelleted by
256 centrifugation at 6,000 g for 5 min and resuspended in 0.1 M Na-cacodylate buffer
257 (pH 7.2) containing 2.5 % glutaraldehyde, 0.075 % ruthenium red (RR) and 100 mM
258 lysine to fix the cells and stain the bacterial capsule with RR (Jacques and Graham
259 1989). After 1 h incubation, cells were washed 3 times with 0.1 M Na-cacodylate
260 buffer and resuspended in 0.1 M Na-cacodylate buffer containing 2 % osmium
261 tetroxide for 2 h. Bacteria were washed 3 times with 0.1 M Na-cacodylate buffer and
262 dehydrated using standard ethanol dilution series, pelleted, embedded in Epon,

263 sliced, thin sections were collected on nickel grids and examined using a Philips CM
264 120 transmission electron microscope. For scanning electron microscopy, *R .equi*
265 were grown on BHI-agar at 37°C for 2 days, scraped off, resuspended in 1 ml fixation
266 solution (4% paraformaldehyde, 2% glutaraldehyde in PBS), transferred on poly-L-
267 lysine-coated coverslips placed in a 24-well plate and incubated for 1 h. Samples
268 were dehydrated through a graded series of diluted ethanol to 100% ethanol,
269 followed by critical-point drying in a CO₂-system and coating with a 2 nm Pt/Pd-layer.
270 Microscopy was carried out on a Philips SFEG XL30 SEM.

271

272 **Statistics**

273 Data are expressed as the mean \pm standard deviations. The significance of
274 differences was assessed with the unpaired, two-tailed Student's *t*-test. Results were
275 termed significant at $p < 0.05$ and highly significant at $p < 0.01$.

276 **RESULTS**

277

278 **The transposome mutant 795 is not mucoid and is defective in capsule**
279 **integrity**

280 In total, 3,300 transposome independent mutants were visually inspected for colony
281 morphology, in particular for the mucoid-glistening appearance characteristic of *R.*
282 *equi* colonies. Approximately 2 % mutants were categorized as 'less mucoid than
283 wild-type' or 'not mucoid'. The *R. equi* mutant 795 possessing the VAP ("795+") was
284 selected for detailed analysis based on its particularly pronounced dry or rough
285 appearance (Fig. 1A). In a broth sedimentation test for clump formation, the mutant
286 bacteria largely sedimented whereas the wild-type bacteria remained largely in the
287 supernatant (Fig. 1B). This suggested a far more hydrophobic surface of the mutant
288 and, hence, possible loss of the extensively hydrated capsule which normally is a
289 prime identifying characteristic of *R. equi* (Prescott, 1991). Genetic complementation
290 of the mutant with cloned *R. equi fbpA* (103+/fbpA- compl) restored the 'mucoid'
291 phenotype of wild-type *R. equi* (not shown).

292 To visualize capsular structures, eosin/nigrosin staining was used which produces a
293 halo around capsule-positive bacteria. Whereas wild-type bacteria had a clear halo,
294 mutant 795 lacked such a halo (Fig. 2), suggesting capsule loss in the mutant. To
295 visualize capsules at the ultrastructural level, bacteria were pre-treated with capsule-
296 binding ruthenium red (Stokes et al., 2004), fixed, and examined by transmission
297 electron microscopy. Most wild-type bacteria had an uninterrupted electron dense
298 surface layer (Fig. 3A), similar to that shown in Garrison et al. (1983). On the other
299 hand, in mutant 795 this surface structure appeared ruptured or missing from large
300 portions of the bacterial surface, and to be profusely distributed on the remaining
301 surface (Fig. 3A). Scanning electron microscopy further revealed the presence of

302 many filamentous structures on 795+ cells which were found much more rarely on
303 103+/fbpA+ (Fig. 3B). Another hallmark feature of mutant 795 was the presence of
304 waxy-like material on the surface of the culture broth supernatant also seen in
305 mycolyltransferase mutants of *Corynebacterium glutamicum* (Brand et al., 2003).
306 These were never observed in used broth from wild-type bacteria (not shown).
307 Determination of the width of the electron transparent layer, consisting of mycolic
308 acid compounds, did not reveal a thicker layer in wild type vs *fbpA* mutant cells.
309 Since the presence of the 'dry' phenotype suggested alterations in cell wall structure
310 that may compromise viability of the bacteria, we analysed growth behaviour in rich
311 (BHI) and in minimal medium using 20 mM acetate as a carbon source. There was
312 no significant difference in growth kinetics between wild-type and 795 bacteria in
313 either medium (data not illustrated).

314

315 **Strain 795 is defective in a rhodococcal *fbpA* homologue**

316 Mutant 795 had only one transposome integration site, as tested by Southern blotting
317 analysis (not shown). To identify the DNA sequences of insertion, the transposome
318 with adjacent host DNA sequences was cloned from genomic 795+ DNA using *KpnI*
319 and the nucleotide sequences were determined. Comparison of the insertion
320 sequence with the known genomic sequences of *R. equi* 103+ using the Sanger
321 Institute's Blast Server (http://www.sanger.ac.uk/Projects/R_equi/) showed that the
322 insertion had occurred within the 1,890 bp predicted open reading frame 285.

323 Nucleotide sequence analysis of ORF0285 revealed a putative ribosomal binding
324 sequence (GAAGGAGAG; pos. 210780-210788) following position -8 of the ATG
325 start codon (pos 210797) and an almost perfectly 42 bp palindromic transcriptional
326 terminator sequence at nucleotides 212704 to 212745 upstream the TGA stop codon
327 (pos. 212686 in Sanger's *R.equi* 103+ genome database). The transposon insertion

328 started with nucleotide number 806 of the ORF0285, i.e., within the codon for amino
329 acid Asp (267) of the 630 amino acids spanning translated sequence.

330 The translated ORF was blasted against the PubMed protein database and
331 homologues with highly significant E-values (*Rhodococcus sp.* HA1 (YP704015): 0.0;
332 *Nocardia farcinica* (YP116390): 0.0; *Corynebacterium glutamicum* (P0C1D7): 5^{-126})
333 were identified (Fig. 4A, sequence of YP704015 not shown). The N-terminus consists
334 of a conserved esterase domain (NCBI-BLAST: COG0627) which is typical for
335 mycoly transferases. A striking homology between the N-terminus of the translated
336 ORF0285 and the three mycobacterial antigen 85 subunits, which are 325 aa to 338
337 aa in length, was found: Between the N-terminal 340 amino acids of the putative *R.*
338 *equi* gene product, 36 % amino acid sequence identity was found with *M.*
339 *tuberculosis* FbpA, 40% with FbpB, and 39 % with FbpC (Fig. 4B) Therefore, the
340 ORF was termed *fbpA*. This nomenclature is not meant to reflect the highest level of
341 relatedness. We choose *fbpA* as the alphabetically first member of the family.

342 Amino acid sequence analysis using the SignalP program
343 (<http://www.cbs.dk/services/SignalP/>) revealed a N-terminal 46 amino acids export
344 signal sequence, suggesting that FbpA is exported, as is *Mycobacterium* FbpA.
345 Further comparison of amino acid sequences revealed the presence of the three
346 amino acid residues of the catalytic triad (Ser₁₂₄, Glu₂₂₈, His₂₆₀) of serine esterases
347 which are also critical for function of mycobacterial FbpC (Belisle et al., 1997). Unlike
348 *Mycobacterium* Fbp-Proteins, but exactly like Fbp-homologues from two other
349 members of the mycolata group, *N. farcinica* and *C. glutamicum*, there was a
350 considerable carboxy-terminal extension (Fig. 4A). The (enzymatic) role of this
351 extension is not known but in case of *R. equi* FbpA contains three 54 amino acid
352 residue tandem LGFP (conserved sequence motif; leucine, glycine, phenylalanine,
353 proline) repeats which may be important for maintaining the integrity of the cell wall

354 (Ramulu et al, 2006). None of the other 12 mycolyl transferase-ORFs in the Sanger
355 *R. equi* 103+ sequence database showed such C-terminal extension, suggesting that
356 this unusual protein would possess a unique activity (the other 12 putative mycolyl
357 transferases are the ORFs 284, 363, 1269, 1418, 1863, 2269, 3018, 4779, 5026,
358 5600, 5697, 6372 in Sanger's *R. equi* 103+ genome database).

359 Genetic complementation of the mutant with cloned *R. equi fbpA* restored the
360 'mucoid' phenotype of wild-type *R. equi* (Fig. 1C).

361 Since loss of mycolyl transferase activity would be expected to lead to an alteration in
362 the pattern of extractable surface glycolipids, we performed thin layer
363 chromatography (TLC) analysis. Using a standard protocol for *Mycobacterium*
364 glycolipid separation previously used to visualize different glycolipid pattern in *R. equi*
365 (Sydor and Haas, unpublished), we could not detect differences between wild-type
366 103+/fbpA+ and *fbpA* mutant lipids except for a lipid which was consistently absent in
367 various preparations from 103-/fbpA+ (Fig. 5). The same was true for other solvent
368 systems (chloroform/methanol/water [65:25:4 or 60:30:8, v/v] or petrol ether/diethyl
369 ether [9:1, v/v]) and modes of development (alpha-naphthol, anthrone/acetic acid,
370 ninhydrin).

371

372 **Phagolysosome formation and phagosome pH are altered in the *fbpA* mutant**

373 To analyse whether phagosome trafficking was affected by the mutation, a
374 microplate phagolysosome formation FRET-assay was used. The higher the relative
375 FRET values, the more phagolysosome fusion has occurred in the macrophage
376 population. Using this assay, 103+/fbpA- was as frequently lysosomal as was
377 103+/fbpA+, but 103-/fbpA- was clearly more efficient at inhibiting phagolysosome
378 formation than the wild-type strain cured of the VAP (103-/fbpA+) (Fig. 6A, p= 0.015).

379 This was surprising, as it could be interpreted as a 'gain-of-function-mutation' of the
380 *fbpA* mutant.

381 A second hallmark of the *R. equi*-containing vacuole (RCV), beyond inhibited
382 phagolysosome formation, is its lack in acidification (Fernandez-Mora et al., 2005).
383 Using a microplate-based assay to quantify macrophage phagosome pH, we
384 determined the pH of RCV in J774E macrophages at 2 h of infection (Fig. 6B).
385 Whereas the average vacuole containing 103+/*fbpA*+ had a pH of 7.2 (\pm 0.27), those
386 containing heat-killed 103+/*fbpA*+ were strongly acidic (pH 5.0 \pm 0.04). RCVs
387 containing 103+/*fbpA*+ or 103+/*fbpA*- were very similar in pH, but those containing
388 103-/*fbpA*+ and 103-/*fbpA*- differed (pH 4.9 \pm 0.25 and 5.7 \pm 0.17, respectively), in
389 agreement with the observed difference in phagolysosome formation data described
390 above.

391

392 **The transposome mutant 103+/*fbpA*- is virulent in macrophage and mouse** 393 **models**

394 To test the potential role of an intact capsule in pathogenesis of *R. equi* infection, we
395 determined bacterial numbers in infected primary bone-marrow derived murine
396 macrophages (BMMs) by a microscopic assay. When identical multiplicities of
397 infection (MOI) were used, wild-type bacteria were taken up in lower numbers than
398 the mutant cells (Fig. 6C, '2 h'). After 24 h, neither 103-/*fbpA*+ nor 103-/*fbpA*- had
399 notably multiplied, but multiplication of 103+/*fbpA*+ and 103+/*fbpA*- was virtually
400 identical, possibly with a somewhat less pronounced multiplication in the mutant
401 considering the initially increased uptake (Fig. 6C).

402 In addition, strains 103+/*fbpA*+, 103-/*fbpA*+, 103+/*fbpA*-, and 103-/*fbpA*- were
403 analysed for virulence in a mouse infection model that has previously been shown to
404 be a valuable model for foal infection (Pei et al., 2006): Bacteria were injected

405 intravenously into CD1 mice at $1 \times 10^6 - 10^7$ bacteria per mouse. Four days later,
406 mice were killed, and bacterial life cell counts in the liver were determined. All
407 103-*fbpA*⁺ and 103-*fbpA*⁻ bacteria were completely cleared, whereas there were still
408 substantial and similar numbers of 103+*fbpA*⁺ and 103+*fbpA*⁻ bacteria left ($10^{5.4 \pm 0.96}$
409 vs $10^{4.8 \pm 0.55}$ bacteria; $p=0.193$), with a slight reduction in 103+*fbpA*⁻ compared to
410 wild-type.

411

412 **Cytotoxicity of macrophage infection with transposome mutant *fbpA***

413 Cytotoxicity of J774E infection with 103+*fbpA*⁻ was similar as that of 103+*fbpA*⁺.
414 Surprisingly, cytotoxicity of 103-*fbpA*⁻ was increased relative to that of wild-type
415 103-*fbpA*⁺ (Fig. 6D).

416 **DISCUSSION**

417

418 In this study, we have shown that a transposome mutation in the gene for mycolyl
419 transferase FbpA resulted in the apparent loss of capsule structure in *R. equi*.
420 Bacterial capsules serve different purposes such as adherence to biotic and abiotic
421 surfaces, resistance to complement-mediated killing, antiphagocytic effects,
422 presentation of a poorly immunogenic (polysaccharide) surface to suppress adapted
423 immune responses, and resistance to desiccation (capsules contain more than 95%
424 of their weight as bound water; Ophir and Gutnick, 1994). Capsules can be major
425 virulence factors in *Escherichia coli*, *Streptococcus pneumoniae* (reviewed in Curtis
426 et al., 2005) and *Haemophilus influenzae* (Moxon and Kroll, 1990). In the case of *R.*
427 *equi*, we have shown an increase of phagocytosis upon loss of capsule structure.
428 This enhanced uptake was clearly detectable yet not impressive and may be the
429 result from unmasking bacterial ligands for binding to macrophage receptors such as
430 the mannose receptor or because of the increased hydrophobicity of the mutant (De
431 la Pena-Moctezuma and Prescott, 1995b). This increased uptake did, however, not
432 result in changed intracellular compartmentation. The major role of the capsule and
433 associated slimes may be to protect these bacteria from desiccation, although we
434 have not directly demonstrated such role. Since rhodococci live mostly in soil,
435 protection from drying out may be a prerequisite for survival not only of virulent
436 strains, since spore formation is not a characteristic of the *Rhodococcus* genus.
437 Capsulation is typical of both virulent and avirulent *R. equi* isolates. In addition to
438 their presumed lack of capsule, 'dry' mutants are interesting because colony variants
439 in mycobacteria can have altered virulence (Pedrosa et al., 1994).
440 The *fbpA* mutant was virulent in a mouse model of infection and multiplied in isolated
441 murine macrophages. This was in contrast to the earlier proposals that the *R. equi*

442 capsule would likely be a virulence factor, possibly by decreasing phagocytosis by
443 macrophages or by inhibiting oxidative killing mechanisms (Ellenberger et al., 1984;
444 Prescott, 1991; Hondalus 1997).

445 Several pieces of evidence showed that the mycolyl transferase *fbpA* mutant lacks a
446 functional capsule: (i) mutant colonies appeared much 'drier' than those of the
447 parent strain; (ii) the mutant had an increased tendency to clump and to precipitate
448 through gravitational force; (iii) transmission electron microscopy using ruthenium red
449 as a capsule dye showed a highly unordered stained polymer around the mutant
450 opposed to a more regular electron-dense material around wild-type bacteria.

451 A previous publication focuses on the process of *R. equi* mutagenesis previously
452 identified a phenotypically-selected 'dry' mutant and identified the mutated ORF as
453 encoding a mycolyl transferase (Ashour and Hondalus, 2003). However, the identity
454 of the ORF was not indicated (*R. equi* has at least 13 mycolyl transferase
455 homologues) and the mutant has not been characterized beyond its 'dry' phenotype.
456 Another study (Pei et al., 2007) has shown that a homologue of antigen 85 in *R. equi*,
457 termed *fbpB* (i.e., another one of the at least 13 mycolyl transferases in the
458 rhodococcal genome), did not change virulence in mice.

459 Four colonial variant forms (A-D) of *R. equi* have been described with A being the
460 classic, highly mucoid colony and D being a small, dry variant. Variant C is an
461 unstable type of dry appearance, sometimes giving rise to type A colonies (Mutimer
462 and Woolcock, 1981). However, the *fbpA*-mutant is stably dry confirmed by repeated
463 cultivation over a long period of time and the re-establishing of the wild-type
464 phenotype by complementation with cloned *R. equi fbpA*.

465 We were surprised that mutant 795, selected for loss of mucoid appearance, should
466 be in a gene coding for a mycolyl transferase, whose product is likely involved in the
467 production of mycolic acid-containing glycolipids, such as cord factor (trehalose

468 dimycolate), rather than in a gene coding for, e.g., carbohydrate metabolism, since
469 the capsule contains large amounts of acidic carbohydrates (Richards, 1994).
470 Whereas the possession of a polysaccharide-containing outermost capsule in virulent
471 mycobacteria is still a matter of debate (Stokes et al., 2004), it has been shown that
472 their cell periphery contains three antigen 85 mycolyl transferases (Belisle et al.,
473 1997), to which we show here that the *R. equi* FbpA is related.

474 Why would the *fbpA* mutant lose its capsule structure? We suggest that a direct or
475 indirect product of mycolic acid chain transfer could be responsible for anchoring the
476 capsule. To be speculative, such a capsule-anchoring product could be (mycolic
477 acid-containing) arabinogalactans which themselves are covalently anchored to the
478 cell wall, which extend into the cell periphery, and whose synthesis is dependent on
479 Fbp proteins in mycobacteria (Sutcliffe, 1997, Takayama et al., 2005). Alternatively,
480 more loosely attached glycolipids, such as trehalose dimycolate, of the cell wall
481 periphery (Sutcliffe, 1997), could anchor substrates through non-covalent
482 interactions. An anchoring role for specific mycolic acids would be reminiscent of
483 capsule anchorage in other systems, e.g., covalent capsule binding to the cell wall
484 (*Streptococcus pneumoniae*) or to other structures, such as phospholipids (*S.*
485 *pneumoniae* type III capsule) (Cartee et al., 2005).

486 *Rhodococcus equi* is thought to have an outer envelope that is unusual among
487 Gram-positive bacteria but is typical of members of the mycolata such as
488 *Mycobacterium tuberculosis* (Sutcliffe, 1997). The filamentous structures that were a
489 characteristic of the 103+/*fbpA*- mutant have been noted previously by Nordmann et
490 al. (1994), but attributed to bacteriophage tails. It seems more likely that they
491 represent shreds of hydrophobic outer envelope material consisting of lipoglycans
492 complexed with mycolic acids.

493 FbpA may have an exceptional position within the group of mycolyltransferases in *R.*
494 *equi* because of its carboxy-terminal extension that is also found in the PS1-Protein
495 of *Corynebacterium glutamicum*. Brand et al. (2003) speculate that this part of the
496 protein plays a role in cell shape formation because deletion of the PS1-coding gene
497 led to a 10-fold increase of bacterial cell volume, which was not however seen in the
498 *fbpA* mutation in *R. equi*. The carboxy-terminus of *R. equi* FbpA includes three LGFP-
499 repeats in the C-terminal region which may be important for anchoring the protein to
500 the cell wall and responsible for maintaining the integrity of the cell wall (Ramulu et
501 al., 2006).

502 We found no obvious changes in the extractable glycolipids by our TLC protocol,
503 likely because of the presence of at least 13 additional mycolyl transferase genes in
504 *R. equi*. For example, *C. glutamicum* possesses 6 mycolyl transferases which can
505 substitute for each other in mycolic acid synthesis (Brand et al., 2003). It is however
506 noteworthy that *C. glutamicum* mutated in the homologous PS1 gene produces waxy
507 surface material in the culture broth which we also observed with 103+/*fbpA*-.

508 In summary, we hypothesize that, among the at least 13 mycolyl transferases of *R.*
509 *equi*, FbpA is a mycolyl transferase involved in capsule anchorage. Its special
510 functional position is highlighted by its conspicuous carboxy-terminal extension (not
511 present in mycobacteria).

512 One of the most interesting observations from this study was the increased
513 intramacrophage multiplication, and the tendency for increased cytotoxicity, higher
514 phagosomal pH, and reduced phagolysosome formation of phagosomes containing
515 103-/*fbpA*- compared to 103-/*fbpA*+. In other words, 103-/*fbpA*- had stronger
516 virulence characteristics than the corresponding wild-type strain. We suggest a
517 hypothesis in which the variant with disturbed capsule structure can more effectively
518 release factors relevant for virulence, such as glycolipids and other cell wall

519 components, and that these factors cause the phenotypes seen. This would not be
520 required in the strains with the VAP, since these may have optimized pathways for
521 secretion that are encoded by VAP genes.

522 The mutation inflicted by the transposome in 103+/fbpA- affects both capsule
523 adhesion and mycolic acid compound synthesis and possibly further phenotypes,
524 making it hard to discuss the role of each of these effects. Still, the fact that overall
525 virulence for mice is unaltered, strongly suggests that the capsule has a negligible
526 role in *R. equi* virulence. This even more so, as mouse clearance studies have been
527 shown to be good indicators of virulence potential when compared to data obtained
528 by parallel foal infection (Giguère et al., 1999).

529

530

531 **ACKNOWLEDGEMENTS**

532 The authors thank Renate Ollig for her expert technical support and the Haas lab
533 members for discussion. This work was supported by a grant from the Deutsche
534 Forschungsgemeinschaft in the *Sonderforschungsbereich* (SFB670) on “Cell-
535 autonomous Defense” (to A.H.) and the Natural Sciences and Engineering Research
536 Council of Canada (to J.F.P.).

537

538 REFERENCES

539

540 Ashour, J., Hondalus, M.K., 2003. Phenotypic mutants of the intracellular actinomycete *Rhodococcus*
541 *equi* created by in vivo Himar1 transposome mutagenesis. J. Bacteriol. 185, 2644-2652.

542

543 Belisle, J.T., Vissa, V.D., Sievert, T., Takayama, K., Brennan, P.J., Besra, G.S., 1997. Role of the
544 major antigen of *Mycobacterium tuberculosis* in cell wall biogenesis. Science 276, 1420-1422.

545

546 Brand, S., Niehaus, K., Puhler, A., Kalinowski, J., 2003. Identification and functional analysis of six
547 mycolyl transferase genes of *Corynebacterium glutamicum* ATCC 13032: the genes *cop1*, *cmt1*, and
548 *cmt2* can replace each other in the synthesis of trehalose dicorynomycolate, a component of the
549 mycolic acid layer of the cell envelope. Arch. Microbiol. 180, 33-44.

550

551 Cartee, R.T., Forsee, W.T., Yother, J., 2005. Initiation and synthesis of the *Streptococcus pneumoniae*
552 type 3 capsule on a phosphatidylglycerol membrane anchor. J. Bacteriol. 187, 4470-4479.

553

554 Curtis, M.A., Slaney, J.M., Aduse-Opoku, J., 2005. Critical pathways in microbial virulence. J. Clin.
555 Periodontol. 32, 28-38.

556

557 De la Pena-Moctezuma, A., Prescott, J.F., 1995a. A physical map of the 85 kb virulence plasmid of
558 *Rhodococcus equi* 103. Can. J. Vet. Res. 59, 229-231.

559

560 De la Pena-Moctezuma, A., Prescott J.F., 1995b. Association with HeLa cells by *Rhodococcus equi*
561 with and without the virulence plasmid. Vet. Microbiol. 46, 383-392.

562

563 Ellenberger, M.A., Kaeberle, M.L., Roth, J.A., 1984. Effect of *Rhodococcus equi* on equine
564 polymorphonuclear leukocyte function. Vet. Immunol. Immunopathol. 7, 315-324.

565

566 Fernandez-Mora, E., Polidori, M., Lührmann, A., Schaible, U.E., Haas, A., 2005. Maturation of
567 *Rhodococcus equi*-containing vacuoles is arrested after completion of the early endosome stage.
568 Traffic 6, 635-653.

569

570 Garrison, R.G., Mirikitani, F.K., Lane, J.W., 1983. Fine structural studies of *Rhodococcus* species.
571 Microbios. 36, 183-190.

572

573 Giguère, S., Hondalus, M.K., Yager, J.A., Darrah, P., Mosser, D.M., Prescott, J.F., 1999. Role of the
574 85-kilobase plasmid and plasmid-encoded virulence-associated protein A in intracellular survival and
575 virulence of *Rhodococcus equi*. Infect. Immun. 67, 3548-3557.

576

577 Herrmann, J.L., O'Gaora, P., Gallagher, A., Thole, J.E., Young, D.B., 1996. Bacterial glycoproteins: a
578 link between glycosylation and proteolytic cleavage of a 19 kDa antigen from *Mycobacterium*
579 *tuberculosis*. EMBO J. 15, 3547-3554.

580

581 Hondalus, M.K., Mosser, D.M., 1994. Survival and replication of *Rhodococcus equi* in macrophages.
582 Infect. Immun. 62, 4167-4175.

583

584 Hondalus, M.K., 1997. Pathogenesis and virulence of *Rhodococcus equi*. Vet. Microbiol. 16, 257-268.

585
586 Jacques, M., Graham, L., 1989. Improved preservation of bacterial capsule for electron microscopy. J.
587 Electron. Microsc. Tech. 11, 167-169.
588
589 Jain, S., Bloom, B.R., Hondalus, M.K., 2003. Deletion of vapA encoding Virulence Associated Protein
590 A attenuates the intracellular actinomycete *Rhodococcus equi*. Mol. Microbiol. 50, 115-128.
591
592 Li, Y., Miltner, E., Wu, M., Petrofsky, M., Bermudez, L.E., 2005. A *Mycobacterium avium* PPE gene is
593 associated with the ability of the bacterium to grow in macrophages and virulence in mice. Cell.
594 Microbiol. 7, 539-548.
595
596 Lührmann, A., Mauder, N., Sydor, T., Fernandez-Mora, E., Schulze-Luehrmann, J., Takai, S., Haas,
597 A., 2004. Necrotic death of *Rhodococcus equi*-infected macrophages is regulated by virulence-
598 associated plasmids. Infect. Immun. 72, 853-862.
599
600 Mangan, M.W., Meijer, W.G., 2001. Random insertion mutagenesis of the intracellular pathogen
601 *Rhodococcus equi* using transposomes. FEMS Microbiol. Lett. 205, 243-246.
602
603 Mutimer, M.D., Woolcock, J.B., 1981. Some problems associated with the identification of
604 *Corynebacterium equi*. Vet. Microbiol. 6, 331-338.
605
606 Nordmann, P., Keller, M., Espinasse, F., Ronco, E., 1994. Correlation between antibiotic resistance,
607 phage-like particle presence, and virulence in *Rhodococcus equi* human isolates. J. Clin. Microbiol.
608 32, 377-383.
609
610 Pedrosa, J., Florido, M., Kunze, Z.M., Castro, A.G., Portaels, F., McFadden, J., Silva, M.T., Appelberg,
611 R., 1994. Characterization of the virulence of *Mycobacterium avium* complex (MAC) isolates in mice.
612 Clin. Exp. Immunol. 98, 210-216.
613
614 Pei, Y., Dupont, C., Sydor, T., Haas, A., Prescott, J.F., 2006. Cholesterol oxidase (ChoE) is not
615 important in the virulence of *Rhodococcus equi*. Vet. Microbiol. 118, 240-246.
616
617 Pei, Y., Parreira, V., Nicholson, V.M., Prescott, J.F., 2007. Mutation and virulence assessment of
618 chromosomal genes of *Rhodococcus equi* 103. Can. J. Vet. Res. 71, 1-7.
619
620 Prescott, J.F., 1991. *Rhodococcus equi*: an animal and human pathogen. Clin. Microbiol. Rev. 4, 20-
621 34.
622
623 Ramulu, H.G., Adindla, S., Guruprasad, L., 2006. Analysis and modeling of mycolyl-transferases in the
624 CMN group. Bioinformation 1, 161-169.
625
626 Ren, J., Prescott, J.F., 2004. The effect of mutation on *Rhodococcus equi* virulence plasmid gene
627 expression and mouse virulence. Vet. Microbiol. 103, 219-230.
628
629 Richards, J.C., 1994. Stereochemical aspects of the antigenic determinants of bacterial
630 polysaccharide: The *Rhodococcus equi* capsular polysaccharides. Carbohydr. Polym. 25, 253-267.
631

- 632 Sekizaki, T., Tanoue, T., Osaki, M., Shimoji, Y., Tsubaki, S., Takai, S., 1998. Improved Electroporation
633 of *Rhodococcus equi*. J. Vet. Med. Sci. 60, 277-279.
- 634
635 Severn, W.B., Richards, J.C., 1999. The structure of the specific capsular polysaccharide of
636 *Rhodococcus equi* serotype 4. Carbohydr. Res. 320, 209-222.
- 637
638 Stokes, R.W., Norris-Jones, R., Brooks, D.E., Beveridge, T.J., Doxsee, D., Thorson, L.M., 2004. The
639 glycan-rich outer layer of the cell wall of *Mycobacterium tuberculosis* acts as an antiphagocytic
640 capsule limiting the association of the bacterium with macrophages. Infect. Immun. 72, 5676-5686.
- 641
642 Sutcliffe, I.C., 1997. Macroamphiphilic cell envelope components of *Rhodococcus equi* and closely
643 related bacteria. Vet. Microbiol. 56, 287-299.
- 644
645 Takai, S., Imai, Y., Fukunaga, N., Uchida, Y., Kamisawa, K., Sasaki, Y., Tsubaki, S., Sekizaki, T.,
646 1995. Identification of virulence-associated antigens and plasmids in *Rhodococcus equi* from patients
647 with AIDS. J. Infect. Dis. 172, 1306-1311.
- 648
649 Takayama, K., Wang, C., Besra, G.S., 2005. Pathway to synthesis and processing of mycolic acids in
650 *Mycobacterium tuberculosis*. Clin. Microbiol. Rev. 18, 81-101.
- 651
652 Tan, C., Prescott, J.F., Patterson, M.C., Nicholson, V.M., 1995. Molecular characterization of a lipid-
653 modified virulence-associated protein of *Rhodococcus equi* and its potential in protective immunity.
654 Can. J. Vet. Res. 59, 51-59.
- 655
656 Vishniac, W., Santer, M., 1957. The Thiobacilli. Bacteriol Rev 21, 195-213.
- 657
658 Yao, J.K., Rastetter, G.M., 1985. Microanalysis of complex tissue lipids by high-performance thin-layer
659 chromatography. Anal. Biochem. 150, 111-116.
- 660
661 Yates, R.M., Hermetter, A., Russell, D.G., 2005. The kinetics of phagosome maturation as a function
662 of phagosome/lysosome fusion and acquisition of hydrolytic activity. Traffic 6, 413-420.

663 **Figures**

664

665 **Fig. 1: Colony morphology of mutant *fbpA* and of wild-type *R. equi*.** (A) Bacteria
666 were grown for 2-3 days at 37°C on BHI agar. Note the glistening, mucoid phenotype
667 of wild-type bacteria (103+/*fbpA*+), whereas mutant 103+/*fbpA*- appears much dryer.
668 (B) Bacteria were grown in BHI broth at 37°C for 16 h in a rotary shaker and then left
669 standing in a tube rack at room temperature for 24 h. Wild-type bacteria 103+/*fbpA*+
670 and 103-/*fbpA*+ and mutant strain 103+/*fbpA*- were used.

671

672 **Fig. 2: Mutant *fbpA* does not possess an intact capsule.** Eosin/Nigrosin staining
673 and phase contrast light microscopy were used to analyse the presence of a halo
674 (white arrowheads) around the bacteria, indicative of a capsule. Top, 103+/*fbpA*+,
675 bottom, mutant 103+/*fbpA*-. Left hand pictures are enlargements of the areas marked
676 by squares. A 100 x oil immersion objective was used for microscopic analysis.

677

678 **Fig. 3: Electron microscopy of *R. equi* wild-type and mutant 103+/*fbpA*-. (A)**
679 Freshly grown bacteria were scraped from a BHI-agar plate and re-suspended
680 directly in fixation buffer. Samples were treated with ruthenium red, fixed and
681 prepared for transmission EM. Different magnifications (see size bars) document the
682 different bacterial appearance. Note the tightly apposed electron dense structure on
683 the surface of wild-type 103+/*fbpA*+, whereas the mutant strain does not possess a
684 coherent electron-dense layer, but rather loosely adherent, filopodia-like structures.
685 (B) Scanning electron micrographs. 103+/*fbpA*+ or mutant 103+/*fbpA*- bacteria were
686 scraped off BHI agar plates and prepared for Scanning EM. Note clumping of
687 103+/*fbpA*- bacteria and their multiple filopodia-like structures that are largely missing
688 from 103+/*fbpA*+ samples.

689

690 **Fig. 4: The gene mutated in *fbpA* codes for a mycolyl transferase. (A)** Amino
 691 acid sequence alignments of mycolyl transferases from different mycolata: *R. e.*
 692 translated ORF0285 of *R. equi*; *N. f.*: *Nocardia farcinica* putative Mycolyltransferase
 693 Nfa1840 (YP116390); *C. g.*: *Corynebacterium glutamicum* PS1-Protein (P0C1D7).
 694 The starting points of the three LGFP-repeats (at aa 434, 488 and 542) are indicated
 695 with arrows. **(B)** Comparison of the deduced amino acid sequence (*R. e.*) with amino
 696 acid sequences of *M. tuberculosis*. The corresponding position of the transposon
 697 insertion is marked with an asterisk. The triangles mark three amino acid residues of
 698 particular importance for enzymatic activity ('catalytic triad'). Identical amino acid
 699 residues in all proteins are shown on black, homologous amino acids on gray
 700 background. FbpA (NCBI accession number P0A4V2), FbpB (NCBI accession
 701 number NP216402), and FbpC (NCBI accession number P0A4V4) are *M.*
 702 *tuberculosis* sequences.

703

704 **Fig. 5: Thin layer chromatography of extractable 103+/*fbpA*+ and 103+/*fbpA*-**
 705 **lipids.** 200 µg of total chloroform/methanol (1:1, v/v) releasable lipid extract from
 706 103+/*fbpA*+, 103-/*fbpA*+, 103+/*fbpA*-, and 103-/*fbpA*- were separated on silica gel 60
 707 plates in chloroform/methanol (9:1, v/v) solvent and developed by short incubation in
 708 CuSO₄/phosphoric acid followed by charring at 250°C.

709

710 **Fig. 6: Analysis of *fbpA*-macrophage interactions**

711 **(A)** Fusion of mutant-containing phagosomes with lysosomes. J774E were infected
 712 with 103+/*fbpA*+, 103-/*fbpA*+, 103+/*fbpA*-, and 103-/*fbpA*-, all of which had been
 713 labelled with ATTO488. Macrophage lysosomes had been loaded with BSA-
 714 rhodamine before the start of the infection. After 30 min of infection, fluorescences

715 were recorded and the degree of FRET was calculated. FRET was set as '1' for
716 103+/fbpA+. The higher the value, the more energy transfer has occurred indicating
717 increased phagolysosome formation. Data are the means and standard deviations
718 from 3 independent determinations. *p*-values were assessed by Student's *t*-test,
719 compared with 103+/fbpA+: 103-/fbpA+, 0.0026; 103-/fbpA-, 0.0447; 103-/fbpA+
720 compared with 103-/fbpA-: 0.0147.

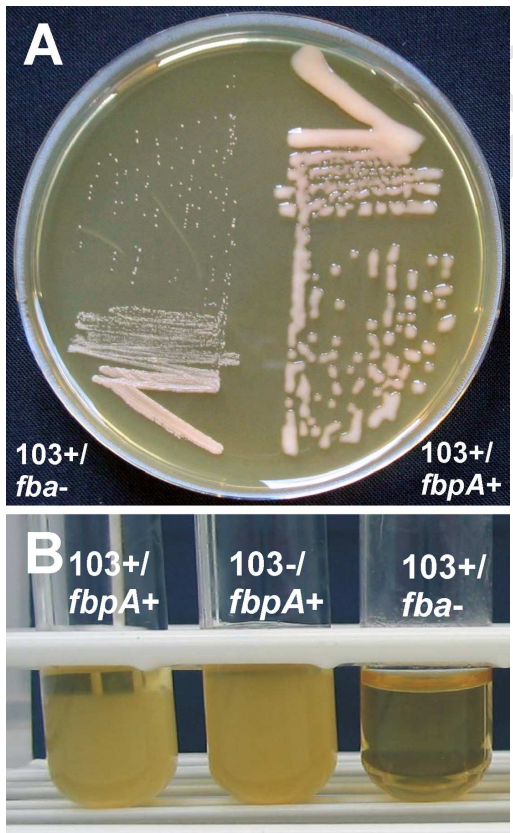
721 **(B)** Determination of pH in phagosomes containing mutant 103+/fbpA-. J774E
722 macrophages were infected with 103+/fbpA+, 103-/fbpA+, 103+/fbpA-, 103-/fbpA-, or
723 heat killed 103+/fbpA+ bacteria, each labelled with two fluorescent dyes to allow
724 ratiometric pH determination. Fluorescence was recorded after 120 min of infection
725 and plotted against pH as determined from the calibration graph, obtained with each
726 particle type in each experiment. At 180 min, nigericin was added to the samples to
727 uncouple the proton gradient over the phagosome membrane, and pH was
728 determined again 20 min later. This pH was then 7.2 (not illustrated), demonstrating
729 correct calibration. Data are the means and standard deviations from 3 independent
730 determinations. *p*-values were assessed by Student's *t*-test, compared with
731 103+/fbpA+: 103+/fbpA+ Δ T, 0.001; 103-/fbpA+, 0.0009; 103+/fbpA-, 0.71; 103-/fbpA-,
732 0.003; 103-/fbpA+ compared with 103-/fbpA-: 0.037.

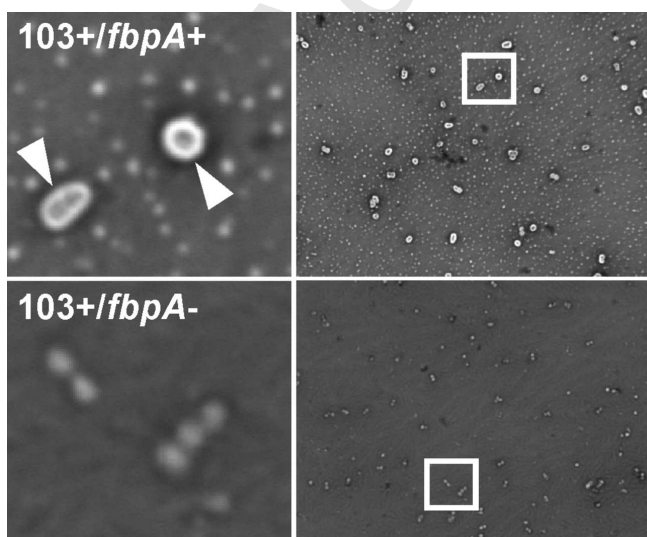
733 **(C)** Multiplication within primary bone marrow-derived macrophages of *fbpA* mutant.
734 J774E were infected with 103+/fbpA+, 103-/fbpA+, 103+/fbpA-, or 103-/fbpA- for 30
735 min, followed by no chase (0 h) or a 24 h chase, and the number of cell-associated
736 bacteria was determined using a fluorescent DNA stain (SYTO13). Data indicate the
737 percentage of infected macrophages with more than 10 bacteria. Data are the means
738 and standard deviations from 3 independent determinations.

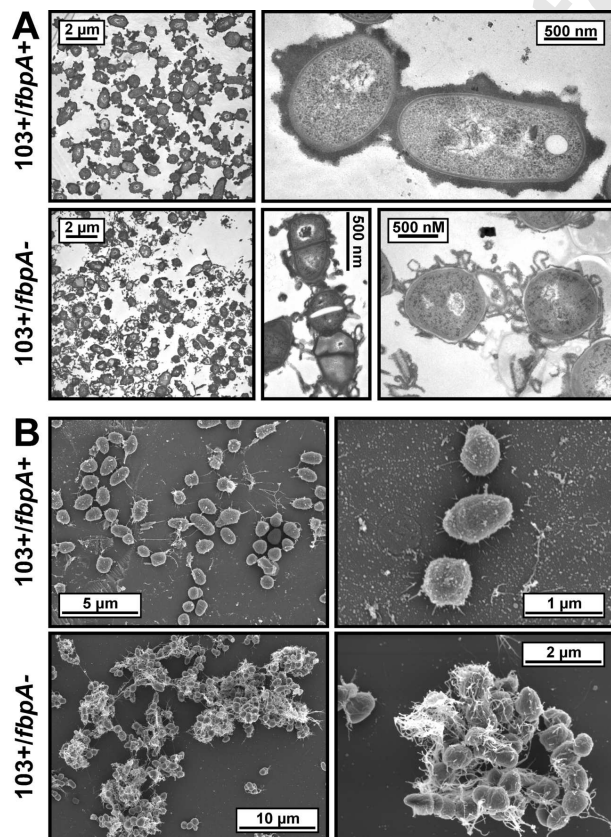
739 **(D)** Cytotoxic effect of infections with mutant *fbpA*. J774E were infected with
740 103+/fbpA+, 103-/fbpA+, 103+/fbpA-, or 103-/fbpA- for 1 h and cytotoxic effect was

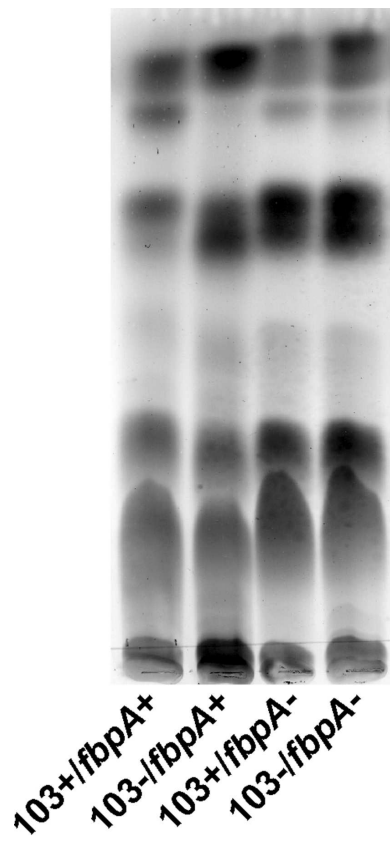
741 quantified using an assay to measure the release of cytosolic lactate dehydrogenase
742 from the macrophages after 24 h of incubation in gentamicin-containing medium.
743 MOI (multiplicity of infection = bacteria per macrophage) was 30. Data are the means
744 and standard deviations of 3 independent determinations. *p*-values were assessed
745 by Student's *t*-test, compared with 103+/fbpA+: 103-/fbpA+, 0.009; 103+/fbpA-, 0.37;
746 103-/fbpA-, 0.041; 103-/fbpA+ compared with 103-/fbpA-: 0.084.

Accepted Manuscript









Accepted Manuscript

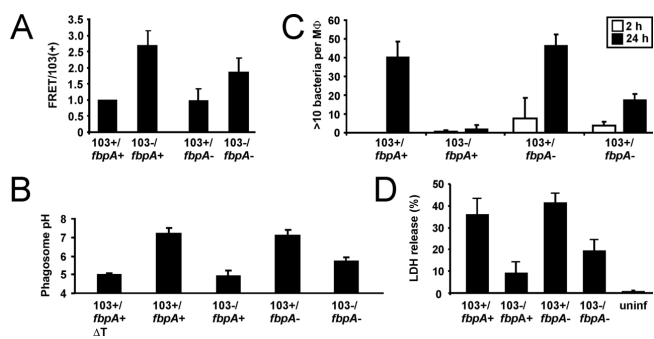


Table1: Bacterial strains, plasmids, and oligonucleotides used in this study

Strain, plasmid, or oligonucleotide	Genotype or characteristics	Source or reference
<i>E. coli</i>		
XL1-Blue	recA1 endA1 gyrA96 thi-1 hsdR17 supE44 relA1 lac [F' proAB lacI ^q ZΔM15 Tn10 (Tet ^r)]	Stratagene
<i>R. equi</i>		
103+/fbpA+	strain with 81 kb virulence plasmid	De la Pena-Moctezuma and Prescott, 1995a
103-/fbpA+	strain cured of the 81 kb virulence plasmid	This study
103+/fbpA-	103+/fbpA+ strain fbpA::211600(EZ::TN Kan-2)	This study
103-/fbpA-	103-/fbpA+ strain fbpA::211600(EZ::TN Kan-2) cured of the virulence plasmid	This study
103+/fbpA-compl	103+/fbpA- strain with pSMT3+fbpA (complemented strain)	This study
Plasmids		
pBluescriptII KS(+)	Amp ^R , αlacZ'	Stratagene
pBluescript + fbpA/Tn	pBluescript with <i>KpnI</i> -fragment of the <i>R. equi</i> -genome containing ORF0285 with the transposon-Insertion	This study
pSMT3	<i>E. coli</i> / <i>Mycobacterium</i> shuttle vector, Hyg ^R	Hermann et al, 1996
pSMT3+fbpA	2417 bp fragment (<i>XbaI</i> , <i>Clal</i>) containing <i>fbpA</i> in pSMT3, used for complementation	This study
Oligonucleotides		
KAN-2 FP-1	5'-ACCTACAACAAAGCTCTCATCAACC-3'	EZ::TN TM <KAN-2> Tnp Transposome TM Kit, Epicentre
KAN-2 RP-1	5'-GCAATGTAACATCAGAGATTTTGAG-3'	EZ::TN TM <KAN-2> Tnp Transposome TM Kit, Epicentre
Tn FP	5'-CTCAAATCTCTGATGTTACATTGC-3'	This study
Tn RP	5'-GGTTGATGAGAGCTTTGTTGTAGG-3'	This study
fbpA FP	5'-CCCTCTAGAGATCCTGAACACTCTGAACGC-3'	This study
fbpA RP	5'-CCCATCGATGTCTTGAAACAGGCTACATACG-3'	This study